Chem Soc Rev

This article was published as part of the

Peptide- and protein-based materials themed issue

Guest editors Rein Ulijn and Dek Woolfson

Please take a look at the issue 9 2010 table of contents to access other reviews in this themed issue

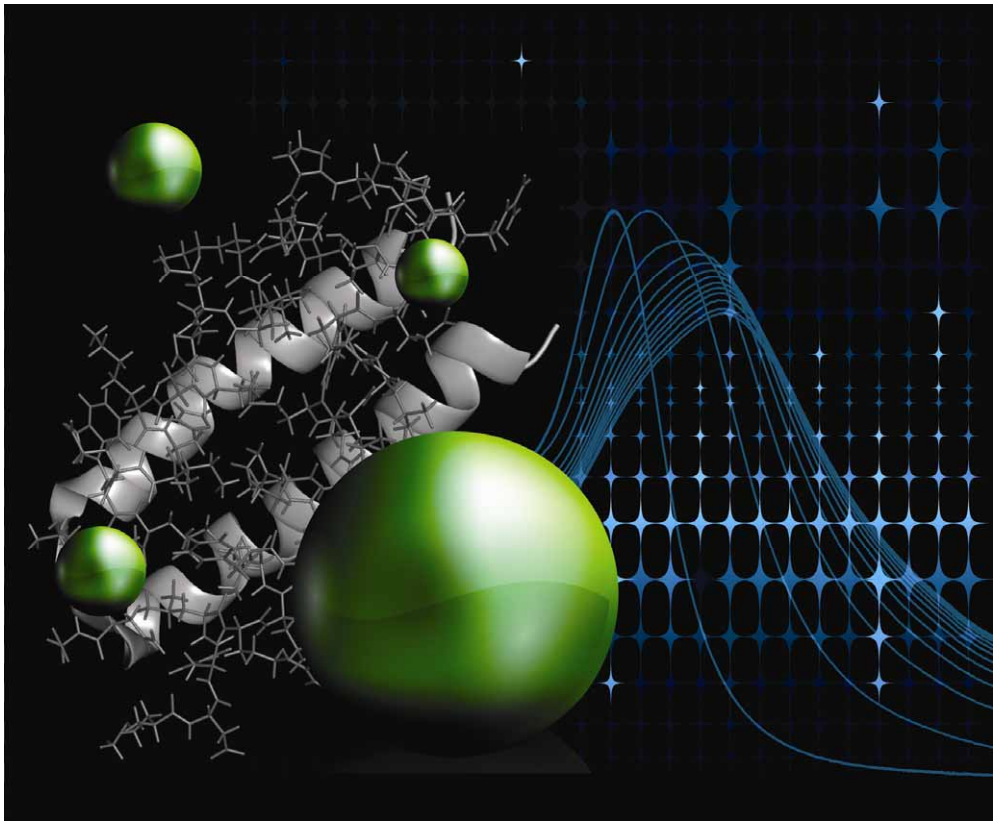

LD spectroscopy of natural and synthetic biomaterials†

Matthew R. Hicks, Jarosav Kowałski and Alison Rodger

Received 4th March 2010
DOI: 10.1039/b912917k

The structural characterization of biomaterials is challenging because they are usually too large for NMR or high resolution mass spectrometry and not well-enough structured for X-ray crystallography. Structural characterization and kinetic analysis for such systems thus has to proceed by collecting complementary data from a wide range of different techniques. This *tutorial review* describes how linear dichroism, a polarized absorbance spectroscopy technique applied to oriented molecular systems, can be used to provide useful data on biomaterials. In particular LD can provide information about relative orientations of sub-units of biomaterials and orientations of the whole biomaterial with respect to an orientation axis. An outline of linear dichroism and a summary of the artifacts to be avoided are followed by a description of how Couette flow linear dichroism has been used for a range of biomaterial systems including: DNA; DNA:ligand systems; cytoskeletal fibrous proteins; synthetic protein fibres; membrane proteins in liposomes; bacteriophage; carbon nanotubes; and peptidoglycan systems.

Linear dichroism spectroscopy: basic principles

Linear dichroism (LD) is a form of absorbance spectroscopy that involves two polarizations of light. LD is defined below, but first consider what absorbance spectroscopy is. A molecule absorbs an incident photon when the energy of its photons corresponds to the difference between energy levels in the molecule

$$\Delta E = h\nu = hc/\lambda \quad (1)$$

Department of Chemistry, University of Warwick, Coventry, CV4 7AL, UK. E-mail: a.rodger@warwick.ac.uk; Fax: +44 (0)2476 575795; Tel: +44 (0)2476 74696
† Part of the peptide- and protein-based materials themed issue.

where h is Planck's constant, λ is wavelength, and c is speed of light, and where the electric field of the photon is in the correct direction to cause the transition to happen. In this article the focus is on what happens when a molecule absorbs photons of visible or ultraviolet (UV) light since the magnitude of the energy of these photons [$(2 - 12) \times 10^{-19}$ J per molecule, λ = 170–800 nm] is that required to rearrange the electron distribution of a molecule.

In practice, in a collection of molecules, the photons absorbed by different molecules will be of slightly different energies. Thus what we measure is a curve, where the signal that is plotted is a measure of the probability that a transition will occur at that energy (or wavelength). Such a plot of the absorbance of light *versus* λ or ν is known as an

Matthew R. Hicks

Matt Hicks is a Senior Research Fellow in Biophysical Chemistry at the University of Warwick, Department of Chemistry. His first degree was in Biochemistry at the University of Bristol. A DPhil in protein–protein interactions at the University of Sussex followed. Subsequent post-doctoral positions in anti-viral peptide drug design and protein–lipid interactions at Sussex and then Warwick University Biosciences led to a Wellcome VIP Fellowship. He then moved to the Department of Chemistry where his current research is varied and includes spectroscopic method development, DNA–drug interactions, fibrous protein structure, peptide–lipid interactions and synthetic biology. He is an Honorary Research Fellow at The University of Birmingham School of Biosciences.

Jarosav Kowałski

Jarosław Kowalski is a Research Fellow at the Department of Chemistry, University of Warwick. He obtained his Master degree in organic chemistry from Akademia Podlaska in Siedlce, Poland, and PhD from the Institute of Organic Chemistry, Polish Academy of Sciences in Warsaw, Poland, in the Molecular Dynamics in the NMR Spectroscopy and Molecular Interactions group. After gaining a PhD degree he worked in the Institute of Organic Chemistry on novel macrocyclic systems. Recently, he has been working on the interactions of DNA with carbon nanotubes and with cyclidene copper(II) and nickel(II) complexes.

absorption spectrum. Absorbance is defined in terms of the intensity of incident, I_0, and transmitted, I, light:[1–3]

$$A = \log_{10}(I_0/I) \quad (2)$$

The Beer–Lambert law for the absorption, A, of light by a sample of concentration C is

$$A = \varepsilon Cl \quad (3)$$

where l is the length of the sample through which the light passes and ε is known as the extinction coefficient; if C is measured in mol dm^{-3} and l is measured in cm, then ε has units of mol^{-1} dm^3 cm^{-1}. ε depends on the identity of the molecules in the sample, their environment and is a function of wavelength, λ.

A linearly polarized light beam is one where all photons have their electric field oscillating in the same plane.[4] Such a light beam will induce a transition in a molecule only if the electric field direction of the photon is at least partially aligned with the direction of net electron motion in the sample (*i.e.* with the electric dipole transition moment). Linear dichroism (LD) is a form of absorbance spectroscopy which makes use of this to determine orientation information about samples. LD is the difference in absorption, A, of light linearly polarized parallel and perpendicular to an orientation axis:[5–7]

$$\mathrm{LD} = A_{//} - A_{\perp} \quad (4)$$

The requirements of an LD experiment are schematically illustrated in Fig. 1. LD requires systems that are either intrinsically oriented or are oriented during the experiment—otherwise the two terms in eqn (4) will on average cancel. The orientation parameter S summarizes the degree of orientation; S, equals zero for unoriented samples and equals 1 for perfectly oriented samples. LD also requires two linearly polarized light beams and some means of measuring the difference in absorbance. LD is useful for biomaterials because many natural and synthetic molecules currently being used as biomaterials are able to be oriented as described below.

Alison Rodger

Alison Rodger graduated from Sydney University with the University Medal for Theoretical Chemistry in 1982. She completed her PhD in 1985 and took up a Beatrice Dale Research Fellowship at Newnham College, Cambridge, together with an Overseas Scholarship from the Royal Commission for the Exhibition of 1851. She next spent six years in Oxford at St. Catherine's and St. Hilda's Colleges, moving to Warwick in 1994. In 2005 she became Professor of Biophysical Chemistry. Her laboratory focuses on developing and implementing UV/visible spectroscopic techniques, particularly linear and circular dichroism, to study structure, function, and dynamics of biomacromolecules in solution.

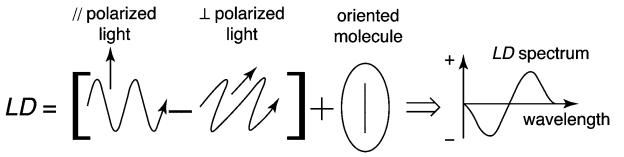

Fig. 1 Schematic illustration of LD. The sine waves indicate the plane in which the electric fields of the // (parallel) and ⊥ (perpendicular) polarized light beams oscillate. Reproduced by permission of the Royal Society of Chemistry from ref. 8.

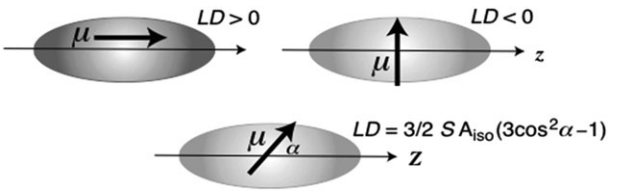

Fig. 2 Schematic diagram of an LD experiment. z is the molecular orientation direction which is the same as the // direction of eqn (4) if the sample is perfectly oriented. $\boldsymbol{\mu}$ is the electric dipole transition moment vector which points along the transition's polarization direction. The formula refers to a uniaxial sample such as a stretched polymer. S is the so-called orientation parameter, $S = 1$ for perfect orientation and $S = 0$ for an isotropic sample. A_{iso} is the absorbance of the corresponding unoriented (isotropic) sample.

The sign and amplitude of the LD of a particular transition depends on the direction along which the light passes through the oriented sample, how well it is oriented and which direction is denoted as 'parallel'. In general, if molecules are perfectly oriented and we measure their absorbance spectrum we have the three possible situations illustrated in Fig. 2. Which one is operative in a given situation depends on how the electric transition dipole moment is oriented with respect to the polarization of the light. They are as follows.

(1) If the direction of the electric transition dipole moment is oriented *parallel* to the orientation direction then only the parallel-polarized photons of light will be absorbed and

$$\mathrm{LD} = A_{//} - A_{\perp} = A_{//} > 0 \quad (5)$$

(2) If the electric transition dipole moment is oriented *perpendicular* to the orientation direction then only the perpendicular-polarized photons of light will be absorbed and

$$\mathrm{LD} = A_{//} - A_{\perp} = A_{\perp} < 0 \quad (6)$$

(3) Between these two extremes, the absorption intensity varies as the cosine square of the angle between the electric field of light and the transition moment as illustrated in Fig. 2.[8]

In this article we shall explore how LD can be used to determine information about biomaterials that is not currently available from any other technique. In the next section a summary of the most widely used orientation methods and artifacts to be avoided are considered. The remainder of the article contains a survey of a selection of types of biomaterials that can be profitably analyzed by LD.

Orienting biomaterials for LD spectroscopy

Which orientation method one should use for LD depends on the sample and the question being asked. Long and relatively

rigid polymers, such as double-stranded DNA or RNA, or molecular assemblies of micrometre dimension, may be oriented by shear flow whereas small molecules require a stronger orienting force. Some molecules which cannot themselves be oriented may be oriented when they bind to another molecule that is oriented. The most commonly used orientation methods for biomaterials are outlined below. A more comprehensive survey is given in ref. 8.

Small molecules oriented on or in polymer films

In 1934 Jablonski proposed that molecules could be oriented by adsorption in anisotropic matrices.[9] If the matrix is a polymer film, when it is mechanically stretched, either before or after the small molecules are added, the included molecules align their long axes preferentially along the stretch direction (see *e.g.*[6]). The best baseline for such an experiment is either that collected for a piece of the same film that has been stretched but does not contain the molecule of interest, or the same film after washing out the analyte molecules or before adding them. In practice, one of two types of films enables one to prepare aligned samples of most molecules: polyethylene for non-polar molecules and polyvinyl alcohol for polar molecules.

Flow orientation of macromolecules

If a rigid or semi-flexible polymer, such as DNA, is dissolved in a solvent then flowed (laminar flow) past a stationary surface at 0.1–3 m s^{-1}, then the molecules experience sufficient shear forces to give a net orientation of the long axis of the polymer along the flow direction. If radiation is incident onto the sample perpendicular to the flow direction, then the absorbance parallel to the flow, $A_{//}$, and the absorbance perpendicular to the flow direction, $A_{\perp}$, are different, so an LD signal may be measured. If the cell components are quartz then data in the visible and UV regions may be collected.

Wada in 1964[10,11] invented a Couette flow cell for LD where the sample is endlessly and stably flowed between two cylinders one of which rotates and one of which is stationary. This is schematically illustrated in Fig. 3. The most recent developments include microvolume Couette flow cells (Fig. 4), which require 25–50 μl of sample rather than the mls of the previous Couette cells, and Peltier temperature control.[12,13] A baseline spectrum must always be subtracted from an LD spectrum.

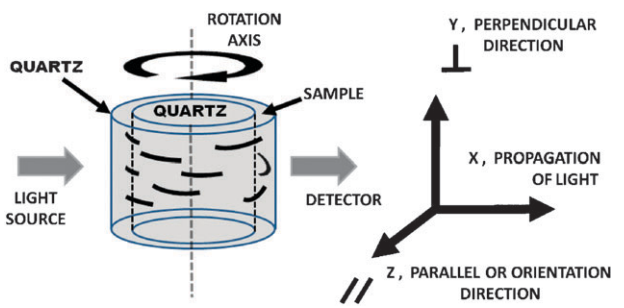

Fig. 3 Schematic of a Couette flow cell showing flow orientation in a coaxial flow cell with radial incident light. {*X*, *Y*, *Z*} form a laboratory fixed axis system.

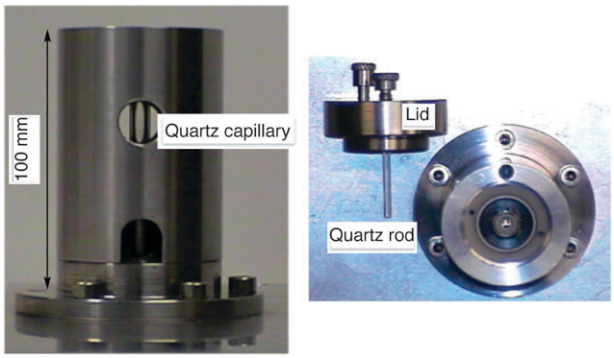

Fig. 4 Microvolume (25–60 μl) outer rotating[12,13] Couette flow cell showing the outer quartz capillary (3 mm inner diameter) and inner quartz rod (2.5 mm outer diameter) making an annular gap of 250 μm.

Flow orientation of liposomes

Lipid bilayer systems have been studied by LD for a long time using either more-or-less dried films (see below) or squeezed gel methodologies. The possibilities for lipid LD were opened up to the more biologically relevant solution phase when Nordén and co-workers showed that unilamellar lipid vesicles (liposomes)—used as model membrane systems with a single bilayer of lipid enclosing a central space—were distorted in shear flow and could be aligned as schematically illustrated in Fig. 5.[14,15] Anything (small molecule or proteins or peptides) bound to the liposome is also aligned.

Orientation by evaporation or assembly

Many molecules can be oriented simply by evaporating them onto a surface that is transparent to the radiation. This method works particularly well for planar aromatic molecules. It also works for membrane bilayer systems. However, since the orientation in such a system is uniaxial, almost always with the unique axis parallel to the normal of the planes of the bilayers, no preferred direction of orientation is observed within the planes. Therefore, the LD is zero when propagating the light through the sample at normal incidence. Instead one has to send in the light at inclined incidence—by tilting the

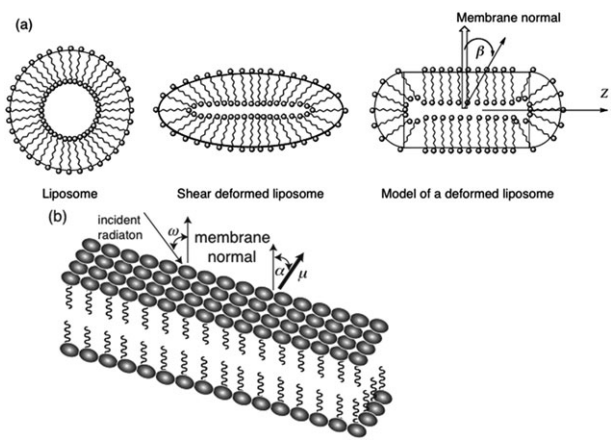

Fig. 5 Schematic diagram of (a) liposomes distorted in shear flow and (b) a tilted membrane. Reproduced by permission of the Royal Society of Chemistry from ref. 8.

sample and a non-standard equation needs to be used as outlined below.

Orientation by evaporation has probably been most extensively used for infra-red studies of lipid bilayers and molecules bound to the bilayers.[16] It is also used for oriented CD studies of membrane proteins.[8] Mono-molecular layers of surface-assembled dye molecules may also be studied in this way.[6]

Some molecules such as Alzheimer's fibres are so large and rigid that simply pipetting them onto a surface from solution may produce a sufficient degree of orientation.[17] In this case the standard equation (see eqn (7) below) should be used since the orientation axis is parallel to the surface not perpendicular to it.

Equations for LD

The equation for the standard fibre geometry LD (*e.g.* DNA, Fig. 2) is

$$\mathrm{LD}^{\mathrm{r}} = \frac{\mathrm{LD}}{A} = \frac{3S}{2}(3\cos^2\,\alpha - 1) \qquad (7)$$

where A is the absorbance, S is the orientation parameter and α is the angle between the orientation axis and the transition moment. By way of contrast, in the cylindrical geometry of the liposome situation

$$\mathrm{LD}^{\mathrm{r}} = \frac{\mathrm{LD}}{A} = \frac{3S}{4}(1 - 3\cos^2\,\beta) \qquad (8)$$

where β is the angle between the normal to the membrane and the transition moment (Fig. 5). The equation for analytes oriented in a membrane that has been tilted at an ω (the angle between the direction of propagation of the light beam and the membrane plane, (Fig. 5)) is:

$$\mathrm{LD}^{\mathrm{r}}(\lambda) = \frac{\mathrm{LD}(\lambda)}{A(\lambda)} = \frac{3S}{2}(3\cos^2\,\alpha - 1) \times \frac{(\cos^2\,\omega)}{[n^2(1 - \cos^2\,\omega/n^2)^{1/2}]} \qquad (9)$$

where α is the angle between the membrane normal and the transition moment, and n is the refractive index. $n \approx 1.33$ for water; 1.5 for glycerol, so the final factor in eqn (9) is $\sim$0.030 for $\omega = 75^\circ$.

Spectral artifacts

Biomaterials are prone to (at least) four types of artifacts which may render LD data misleading.

Sample loading

Many biomaterials are quite viscous. In such cases the very act of pipetting the sample into a sample holder or the assembly of a microvolume Couette flow LD cell can induce alignment in the sample. In some cases simply cutting a pipette tip so that the orifice increases in size to $\sim$2 mm can remove the problem.

Light scattering samples

Many of the samples for which we wish to measure LD data are of comparable size to the wavelength of light. As a result they often scatter light significantly. Furthermore, as well as differentially absorbing the two incident polarizations of light (the intrinsic LD signal), they may also differentially scatter the light. If at all possible, one should avoid scattering occurring rather than trying to correct for it. Its presence is usually indicated by a sloping baseline outside absorbance bands. In general, scattering can be reduced either by reducing the size of the particles or collecting a high percentage of the scattered photons. The latter can often be achieved by either having a wide angle photomultiplier tube on the spectrometer, or placing the sample very close to the photomultiplier tube, or having a collecting lens close to the sample to refocus the scattered light onto the PMT.

However, these options may either be insufficient or not available. In general we may write for LD

$$\mathrm{LD}^{\mathrm{Observed}} = \mathrm{LD}^{\mathrm{Absorbance}} + \mathrm{LD}^{\mathrm{Scattering}} \qquad (10)$$

We generally only want the absorbance contribution. Nordh *et al.*[18] showed that a simple empirical correction can often be subtracted from the observed LD spectrum to remove the sloping baseline[19]

$$\mathrm{LD}^{\mathrm{Scattering}} = \alpha\lambda^{-k} \qquad (11)$$

as illustrated in Fig. 6.

Stray light

In addition to any light scattering from the sample, so-called 'stray light' from anywhere in the system, may cause additional artifacts. Stray light is particularly an issue at lower wavelengths for xenon lamp instruments where the light of the correct wavelength has low intensity. In such a case, a significant percentage of the light that does reach the photomultiplier tube may be stray light rather than light of the correct wavelength that has passed through the sample.

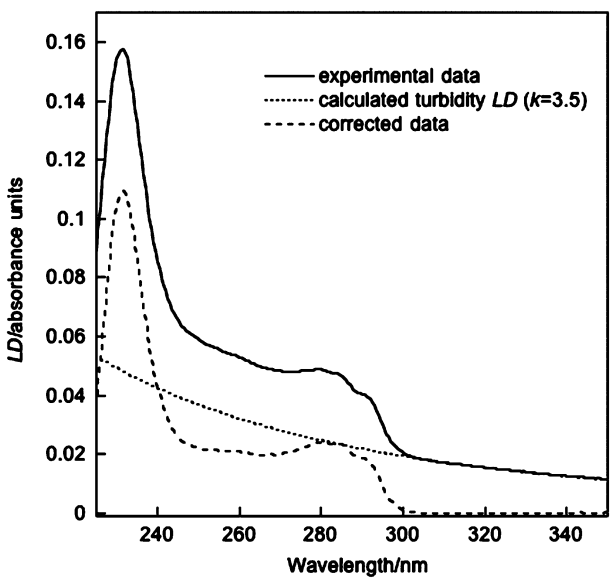

Fig. 6 A method of light scattering[18] correction applied to an LD spectrum of polymerized tubulin (Fig. 18): the experimental data (—); the calculated turbidity LD with α determined by rescaling the curve at 320 nm where there is no intrinsic absorbance (---); and the corrected data (– – –).[20]

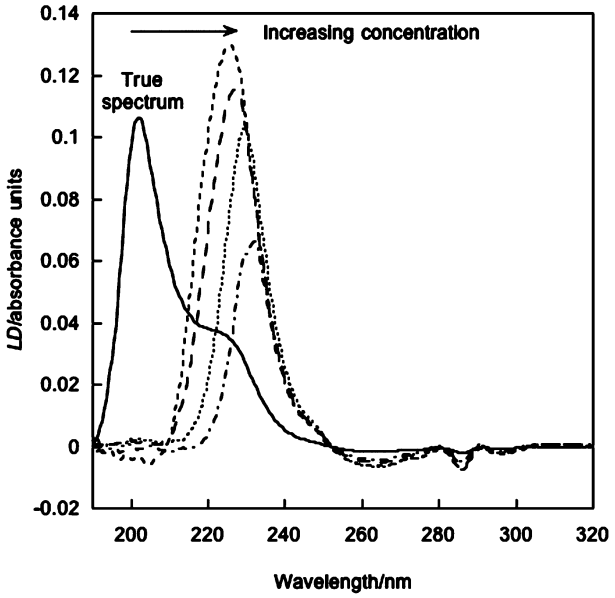

Fig. 7 Far UV LD spectra showing the apparent shift to shorter wavelength of the maximum signal as the concentration of strongly light scattering F-actin fibres is reduced. F-actin concentrations 93, 74, 62, 53 and 12 μM (the true spectrum, solid line). The high tension voltage of the instrument remained below 600 V (usually considered 'safe') throughout the experiment.[19]

However, all photons get counted and are assumed to be unabsorbed photons of the monochromator's wavelength, causing the photomultiplier to 'believe' there is less absorption or LD at the monochromator wavelength than there really is. If the spectrum is 'true' it will follow the Beer–Lambert Law (eqn (3)). A sharp drop off in intensity on the low wavelength side of a band (Fig. 7) is often indicative of this problem.

Absorption flattening

The phenomenon of so-called absorption flattening is a suppression of the absorbance signal in regions of high absorbance in non-homogeneous samples causing the Beer–Lambert law to break down. The same issues apply to LD.[21,22] Because the problem arises for inhomogeneous samples, often the overall intensity of light collected by the PMT seems satisfactory but a true signal is not being obtained. Membrane samples such as liposomes (Fig. 5) are particularly problematic since the analytes often assemble within a liposome, which are themselves a partition of the solution. Chromophores are also close-packed in fibres and the same problem arises. Unfortunately, the absorption suppression cannot always be avoided. In such cases methods such as those of ref. 21 can be used to correct measured data.

LD of DNA and DNA–ligand systems

In order to understand the LD of any system and to interpret it to give structural information, one needs to understand at least something about the intrinsic absorbance spectroscopy of the units that make up the system. In the case of DNA this is the DNA bases.

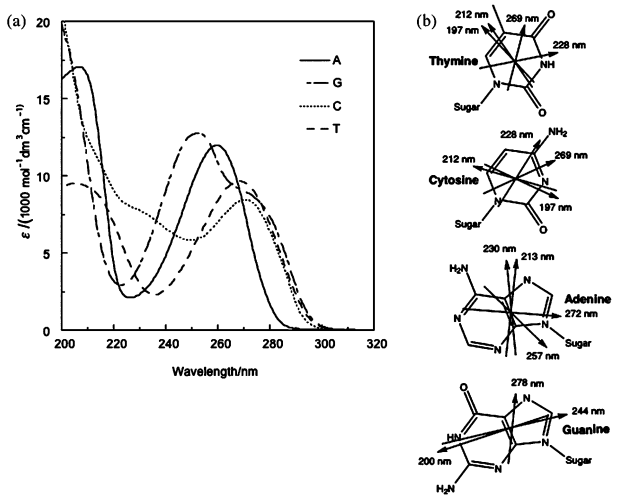

Fig. 8 (a) UV spectra of the DNA nucleotides deoxyadenosine 5′-monophosphate (A), deoxyguanosine 5′-monophosphate (G), deoxycytidine 5′-monophosphate (C), and thymidine 5′-monophosphate (T) (that of uracil is very similar). (b) Probable transition polarizations for UV transitions of adenine,[24,25] guanine,[26] cytosine,[27] and thymine.[28]

Absorbance spectroscopy of DNA bases

The absorption, and hence LD, spectra of nucleic acids in the easily accessible region of the spectrum (down to ~180 nm) are dominated by the $\pi \rightarrow \pi^*$ transitions of the purine and pyrimidine bases.[23] The absorbance spectra of the DNA bases thymine (T), adenine (A), guanine (G), and cytosine (C) and the current best estimates of their transition polarizations are illustrated in Fig. 8.

B-DNA LD

The $\pi \rightarrow \pi^*$ transitions of DNA are all polarized in the plane of the bases, so when the bases are assembled approximately perpendicular to the helix axis of B-form DNA the transitions are all polarized perpendicular to the helix axis. This means the transition moments are perpendicular to the *z*-axis of Fig. 2, so LD < 0. If the B-DNA bases were oriented perfectly perpendicular to the helix axis, as in an idealised structure of B-DNA, the LD of B-DNA would simply be the negative of the absorbance spectrum. In practice this is not quite true as illustrated in Fig. 9, since the bases are tilted. The slope of the reduced LD, LD^r, has been used to determine that in solution the bases of B-DNA in solution lie at an average angle of ~80° or even less from the helix axis[23] (though we typically assume 86° in a calculation).[29]

The shortest piece of DNA that can be flow-oriented is about 250 base pairs. DNAs of this length, however, give very weak LD signals. To use LD quantitatively, lengths should be 800 or more base pairs.

DNA–ligand LD

When ligands bind to DNA, the LD signals at the ligand absorbance wavelengths can be used to determine the ligand orientation on the DNA—as long as we know the ligand transition polarizations.

Molecules such as ethidium bromide that intercalate between DNA bases push the base pairs apart by ~3.4 Å

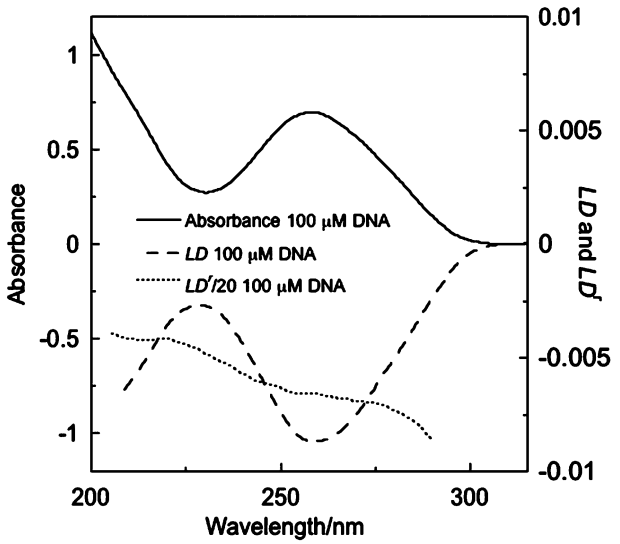

Fig. 9 Absorbance, LD and LD^r spectra of calf thymus DNA (100 μM) in, respectively, a 1 cm path length cuvette and a 1 mm path length Couette flow cell. $LD^r \approx -0.15$, so $S \approx 0.05$.[8]

and unwind the helix by up to 36°, thus both lengthening and stiffening DNA so increasing the DNA base LD. The transitions of the intercalator itself give extra negative LD intensity (Fig. 10a) indicating that its transitions are approximately parallel to the DNA bases. By way of contrast, the long axis polarized transition of the minor groove binder Hoechst 33258 gives a positive signal at 350 nm (Fig. 10b).

Determining the orientation parameter *S* for DNA

In practice, for macromolecular systems, *S* is usually determined more or less reliably by empirical means either by using known maximum LD^r values (perhaps from a parallel experiment assuming the DNA orientation does not change), or by calibrating with a probe dye whose binding geometry is known and whose spectroscopy is in a different place from that of the DNA and any other ligand of interest.[30,31] By assuming $\alpha = 86°$ for the intrinsic DNA LD of the absorption at 260 nm, a sufficiently good estimate of *S* is often obtained from eqn (7) to allow the application of the same equation to determine α values for ligand transitions.

LD to determine DNA bending or stiffening

The magnitude of *S* can be used to provide information about the length, flexibility, or bendability of DNA (or any other polymer or fibre) or about the introduction of kinks into DNA. If *S* increases as the result of some change imposed on the system (such as the addition of a DNA-binding ligand), then the DNA has become more oriented. This generally means it is lengthened, or stiffened (or both) or some bend or kink has been removed.[32–35]

DNA superstructures

The LD of any supramolecular aggregate with local uniaxial symmetry (*e.g.* a helix) is obtained as the sum of the squares of the absorption vectors projected on to the orientation axis of

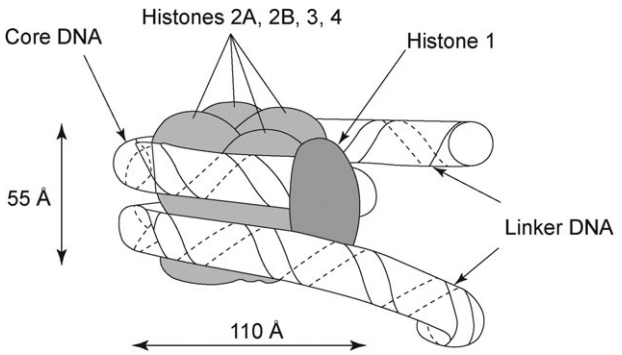

Fig. 11 The nucleosome. Reproduced by permission of the Royal Society of Chemistry from ref. 8.

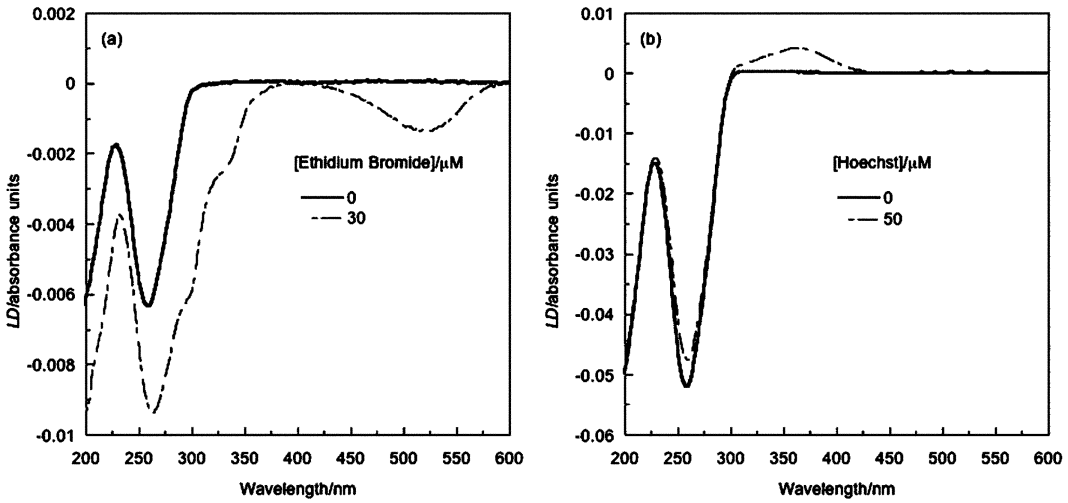

Fig. 10 Linear dichroism in a 1 mm path length Couette flow cell of (a) calf thymus DNA (200 μM, 20 mM NaCl, pH = 7) and ethidium bromide (concentrations shown in the figure); (b) calf thymus DNA (1000 μM, 20 mM NaCl, pH = 7) and Hoechst 33258 (concentrations shown in the figure).[8]

the aggregate minus the sum of the squares of the projections perpendicular to this axis.[36] For supercoiled DNA (in plasmids or chromatin, Fig. 11), the LD is:[8,36]

$$LD^r = \frac{3}{2}S(3\cos^2\alpha - 1)\left(\frac{1}{2}\right)^N \prod_{i=0}^{N}(3\cos^2\Psi_i - 1) \qquad (12)$$

where S is the usual orientation parameter (in this case of the superstructure), α is the angle the transition moment of interest makes with the local orientation axis, Ψ_i is the pitch angle of the superhelix, N is the order of supercoiling: $N = 0$, no supercoil ($\Psi_0 = 0$); $N = 1$ a first supercoil, with pitch angle Ψ_1; $N = 2$ a supercoiled supercoil with pitch angle Ψ_2; and so on. The effect of increasing the order of supercoiling is thus to decrease the total LD. In addition, since supercoiling generally makes a particle shorter, the effective orientation will probably be worse though the DNA does also get stiffer which increases S. This is an application of LD that has potential to be very useful in the biomaterial field but has only had limited use to date.

Chromatin structure

One of the most important biomaterials for eukaryotic living systems is chromatin, the DNA–histone protein complex that accommodates the DNA in the eukaryotic cell nucleus. The human genome contains some 3×10^9 DNA base pairs corresponding to a linear length of DNA of about 1 m located in 23 chromosomes. To accommodate these giant DNA pieces in an eukaryotic cell nucleus of about 5 μm in diameter, efficient packing is required: this packing takes place at a number of levels—each could be represented by one factor in the superhelix product describing LD in eqn (12).[37]

LD of protein systems

Attempts to use LD to study protein systems usually encounter one of two problems: either the system is difficult to orient (as is certainly the case for globular proteins); or, once oriented, the structure surrounding the oriented protein, such as a cell membrane or a filamentous aggregate, that is required to create orientation may give rise to artifacts as discussed above. These problems are, however, generally surmountable and LD has been used to good effect to determine orientations of chromophores, mobility of particular centres, and for studying ligand binding, DNA–protein interactions, fibre assembly, and protein insertion into membranes. Some examples are given below after a summary of protein spectroscopy.

Protein UV spectroscopy

UV spectra of proteins are usually divided into the 'near' and 'far' UV regions. The near UV in this context means 250–300 nm and is also referred to as the aromatic region (though transitions of disulfide bonds (cystines) also contribute to the total absorption intensity in this region). The far UV ($<$250 nm) is dominated by transitions of the peptide backbone of the protein; transitions from some side chains also contribute in this region. Fig. 12 summarizes the most commonly seen protein transitions together with their polarizations.

The lowest energy transition of the peptide chromophore is one from a non-bonding orbital to an anti-bonding π orbital: an n → π* transition analogous to that in ketones. The next transition is a π → π* transition. The longest wavelength n → π* transition is of low intensity ($\varepsilon \approx 100$ mol^{-1} dm^3 cm^{-1}) and occurs at about 210–230 nm (depending mainly upon the extent of hydrogen bonding of the oxygen lone pairs). The π → π* transition ($\varepsilon \approx 7000$ mol^{-1} dm^3 cm^{-1}) is centred at ~190 nm. These transitions are schematically illustrated in Fig. 12.

Fibrous proteins: cytoskeletal proteins

The cytoskeleton in both prokaryotic and eukaryotic cells is dependent on the rapid and controlled assembly and disassembly of polymers (fibres) whose monomeric units are themselves folded proteins. The structures of the monomers change little if at all when they form the fibres. In some cases a single linear polymer forms, in other cases further assembly into bundles (thicker fibres) of some kind occurs. Some protein fibres, such as tubulin, assemble to form more complicated structures directly. Monomeric proteins before polymerization have no flow LD signal, thus they provide no background signal to interfere with attempts to follow kinetics of fibre assembly, disassembly and reorganisation. The possibilities of LD spectroscopy can be illustrated by looking at the bacterial homologue of tubulin, FtsZ, and tubulin itself.

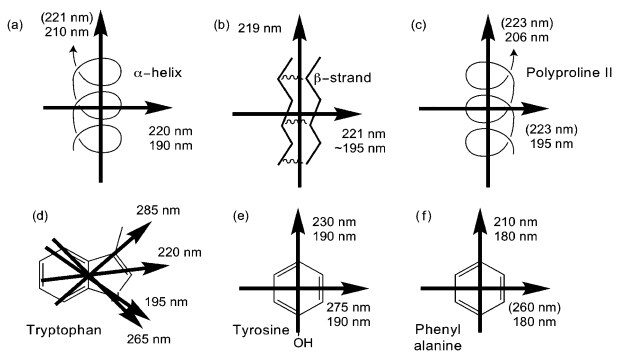

Fig. 12 UV transition polarizations for (a) α-helix, (b) β-sheet, (c) polyproline II helix,[15] (d) tryptophan,[38] (e) tyrosine,[38,39] and (f) phenyl alanine. Transitions indicated in parentheses are weak.

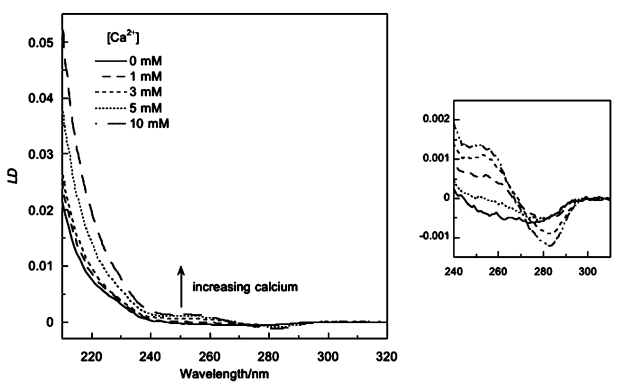

Fig. 13 FstZ (11 μM) polymerization in the presence of $MgCl_2$ (10 mM) and varying amounts of Ca^{2+} (50 mM MES buffer, pH 6.5, 50 mM KCl, 0.1 mM EDTA and GTP (0.2 mM)). The GTP region is expanded on the right.

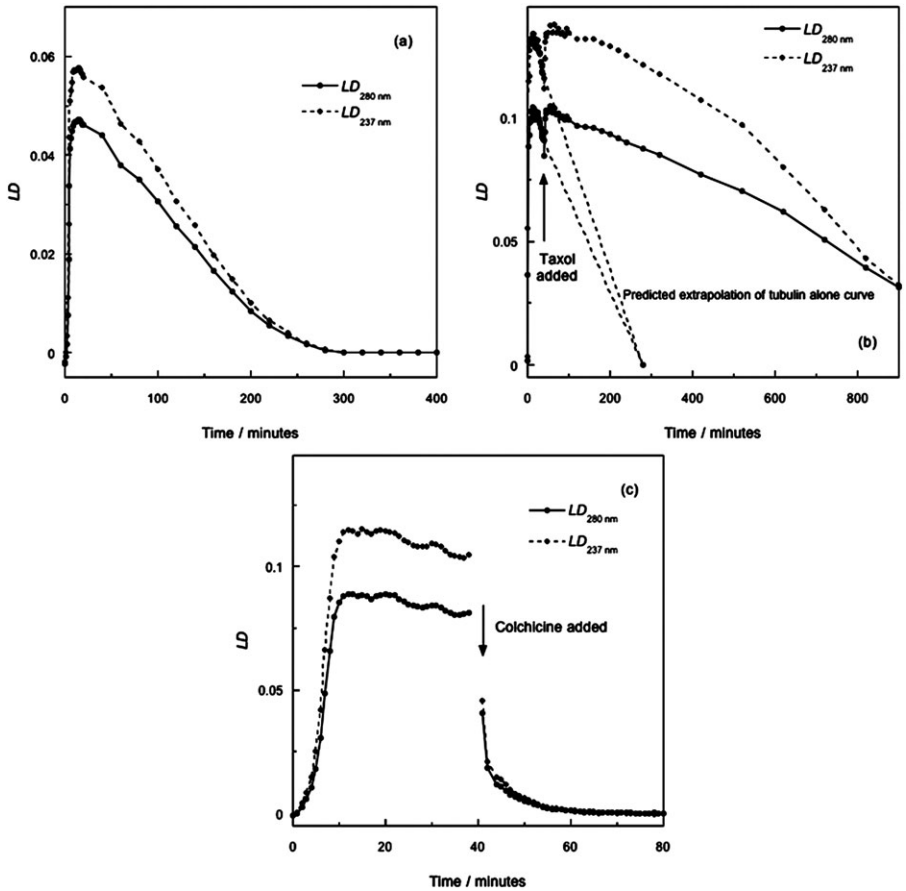

Fig. 14 Capillary LD at two absorbance wavelengths of tubulin polymers (28 μM monomer) at 37 °C: (a) tubulin only; (b) tubulin before and after the addition of taxol (final concentrations 25.5 μM and 18.2 μM, respectively); (c) tubulin before and after the addition of colchicine (final concentrations 25.5 μM and 18.2 μM, respectively).[41]

FtsZ is a bacterial protein that polymerizes to form the so-called Z-ring which then contracts and pulls in the cell membrane to enable one cell to divide into two daughter cells. The complex is thus one of nature's most effective biomaterials in terms of structure and structure change. *In vitro* (and presumably *in vivo*), FtsZ polymerizes to form linear polymers or protofilaments on the seconds timescale when GTP (guanine triphosphate) and Mg^{2+} are present. The protofilament LD spectrum for *E. coli* FtsZ is the 0 mM Ca^{2+} spectrum of Fig. 13. Upon addition of Ca^{2+}, the FtsZ protofilaments bundle together[40] tilting the guanines from horizontal causing the 260 nm LD to become positive. The protein YgfE performs the same role as the calcium ions but at more biologically realistic concentrations.[40] LD is currently the only technique that can follow such a reorganisation of the components of this complicated molecular system in real time.

The eukaryotic protein tubulin is also a polymer of protein monomers with a GTP between each monomer unit. As its name implies, tubulin forms tubules. The proteins α-tubulin and β-tubulin first dimerize, then assemble into hollow cylindrical filaments. Rather than forming a Z-ring, tubulin polymers radiate from the centrosome of a cell to attachment sites just under the cell membrane during cell division. Microtubules also play a role in moving cells and organelles and interact with motor proteins. They are thus very attractive dynamic drug targets. LD is the ideal (and perhaps only) technique to follow the kinetics of processes such as the fibre assembly and disassembly as illustrated in Fig. 14.[41] The rates are the same in the aromatic region (280 nm) and backbone region (237 nm) which means that the backbone and side chains adopt their final orientation simultaneously. The high concentrations of tubulin needed to initiate polymerization mean that the data are only reliable down to about 235 nm as the sample absorbance is too high below this point. The polymerization in the absence (Fig. 14a) and presence (Fig. 14b) of the taxol illustrates the stabilisation effect of taxol on the microtubules. Colchicine (which is used in the treatment of gout), by way of contrast, results in tubulin depolymerizing (Fig. 14c) by preventing the monomers from polymerizing.

Fibrous proteins: synthetic biomaterials

Self-assembled α-helical fibres. Interest in the design of peptide-based fibrous materials is growing, and indeed has motivated the production of this special issue. Peptide-based fibrous materials open possibilities to explore fundamental aspects of peptide self-assembly, and to exploit the resulting structures, for example, as scaffolds for tissue engineering. Here we illustrate how LD can be used in this type of work

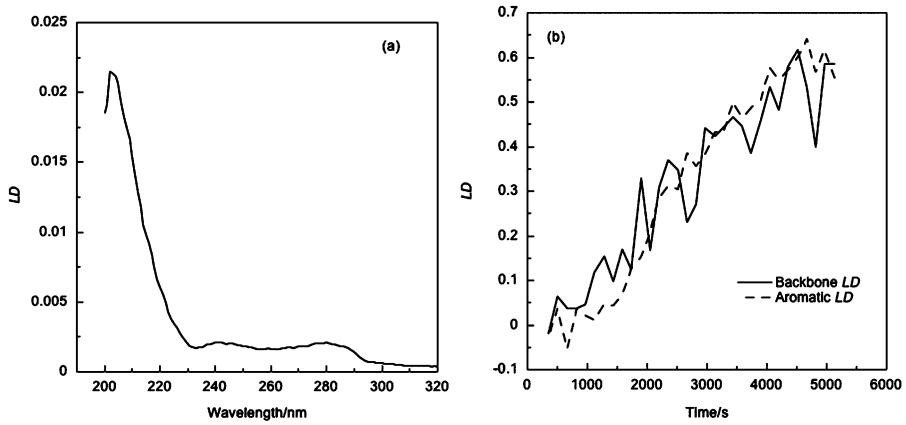

Fig. 15 (a) Linear dichroism spectrum of a mature SAF (100 μM of each of KIAAPKQKIASLKQEIDALEYENDALEQ and KIRRPKQKNARLKQEIAALEYEIAALEQ). (b) Growth of backbone and aromatic LD signals as a function of time with data normalized to 1 at long time.

using data on a rationally designed α-helical coiled-coil fiber comprising two peptides that assemble on mixing.[42] The fibers are formed *via* a nucleation and growth mechanism as follows: the two peptides combine rapidly (<seconds) to form sticky ended, partly helical heterodimers; a lag phase follows, which is of the order of tens of minutes depending on peptide concentration; a critical nucleus comprising 6–8 partially folded dimers then forms with growth being linear in dimers; subsequent fiber growth occurs in hours through both elongation and thickening. In this case the two component peptides are a self-assembling fiber (SAF) system, which comprises two complementary, *de novo* designed, leucine-zipper peptides, each 28-residues long.[43]

SAFs exhibit an LD spectrum when shear aligned. The spectrum (Fig. 15a) indicates that both the peptide backbone and the tyrosine residues are aligned. By recording LD spectra during fibrillogenesis, a fractional completion curve can be generated (Fig. 15b). The LD data show an increase in the alignment of both the Tyr residues and the backbone sometime after the initial increase in the circular dichroism signal reported in ref. 42. This is consistent with the peptides first folding then assembling into long fibres. The circular dichroism kinetics show a final slow increase in secondary structure during which time the LD intensity continues to increase confirming that the fibres are continuing to develop during this time period.

Self-assembly of Sup35 yeast prion fragment, GNNQQNY. Amyloid-like fibrils can be formed by many different proteins and peptides. These fibres have very similar structural characteristics to those of amyloid fibrils that are deposited in a number of protein misfolding diseases including Alzheimer's disease and the transmissible spongiform encephalopathies. The elucidation of two crystal structures from an amyloid-like fibril-forming fragment of the yeast prion, Sup35, with sequence GNNQQNY, has contributed to knowledge regarding side-chain packing of amyloid-forming peptides. Both structures share a cross-β steric zipper arrangement but vary in the packing of the peptide, particularly in terms of the tyrosine residue. Linear dichroism enabled which one was relevant in solution to be determined. LD also showed (Fig. 16) that a change in the orientation of the tyrosine residues occurred over time suggesting a structural rearrangement occurs as crystals form.[17]

In general for such fibres, LD can be used to give information regarding the orientation of the π to π* transitions in the peptide bond of β-sheet structures that absorb light around 195 nm. The sign of the LD signal at this wavelength identifies the orientation of β-strands relative to a larger structure. In this case (Fig. 16) the peptide fibre is consistent with the cross-β structure shown previously.[44] Furthermore, the LD signal can be measured in real time to follow the kinetic processes that occur during fibre formation and to identify changes in backbone and aromatic side chain orientation during this process. In this case the aromatic LD (Fig. 16b) shows two maxima at 278 nm and 286 nm. This is evidence of exciton coupling of the tyrosine transitions, which occurs only when the tyrosines are in close proximity. The positive signals appearing at the same time around 230–240 nm are also consistent with exciton coupling of tyrosine transitions.[8] Furthermore, there is a change in the sign of the aromatic LD signal over time (when the sloping baseline due to light scattering is taken into consideration) indicating that the tyrosine side chain changes its orientation early in the kinetics process.

Membrane proteins

Membrane proteins and peptides are peripherally associated with or embedded within the cell's bilayer membranes. They play key roles in cells as ion channels and in cell signalling systems. The malfunctioning of these units is directly linked to diseases, such as cancer, diabetes, and arteriosclerotic disease, *etc*. Membrane proteins are therefore important drug targets and membrane peptides are also drug candidates; however, we have only a very limited understanding of their structure, function, and intermolecular interactions in their membranes. Despite their importance (~1/3 of proteins coded by the human genome are membrane proteins), we know comparatively little about membrane proteins and membrane peptides because they are very challenging to study. This means that we have made little progress in using membranes and membrane proteins as biomaterials of any kind. Here we give a few

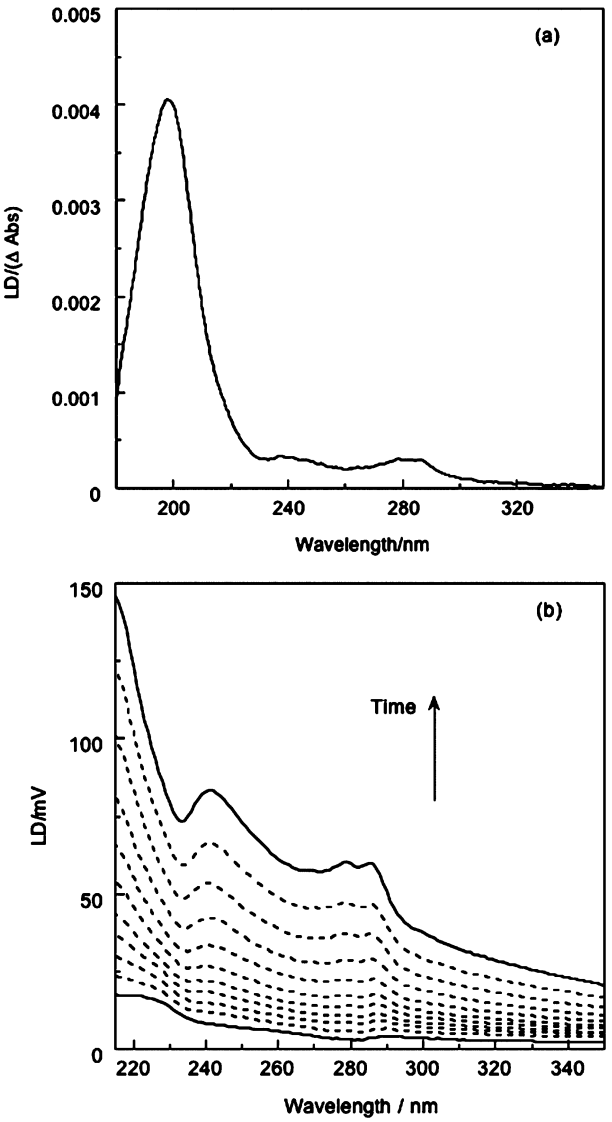

Fig. 16 (a) LD spectrum of mature GNNQQNY fibre sample at 0.2 mg ml^{-1}. A strong π to π* transition around 195 nm is consistent with the formation of cross-beta structure. There are aromatic signals around 280 nm resulting from ordered tyrosine side chains in the structure. (b) Kinetics of fibre/crystal formation by GNNQQNY at 2 mg ml^{-1}. Spectra were measured at 8 minute intervals increasing in magnitude with time. Careful inspection at 280 nm shows the aromatic region inverts its sign at early time points. Units are in mV as the data were collected at the Astrid Synchrotron.[45,46] LD = 3.3×10^{-4} per mV.

examples to show how LD can be used to determine how membrane peptides interact with a membrane both as a snap shot and as a function of time. We anticipate that such applications will become of more importance to the biomaterials field in the future including photosynthesis mimicking systems.

LD of membrane peptides in liposomes. LD is an extremely attractive technique for probing whether or not a species such as a proposed trans-membrane antibiotic peptide binds to a given membrane. When the secondary structure of the peptide is known (*e.g.* α-helical or β-sheet) from *e.g.* CD, then its orientation can be approximately determined from the sign of the LD. If *S* is known then the orientation angle of the peptide can be determined more accurately. LD is currently the only technique that can provide this information in solution phase.

The possibilities are illustrated in Fig. 17 for a simple α-helical peptide and a β-strand peptide. To understand what the spectra mean we consider eqn (8) and the transition polarizations summarised in Fig. 12. For peptides tilted at an angle of 54.7° from the membrane normal we expect to see no LD just as if the peptide were not bound. Fig. 18 summarizes what is expected for α-helices and β-strands inserted in the membrane. The Fig. 17a α-helix is therefore inserted into the membrane in a trans-membrane manner, whereas the β-strand of Fig. 17b is lying flat on the surface of the membrane. It should be noted that the 208 nm α-helix negative band is dominated by its neighbours so appears as a small dip between two larger positive signals.

Gramicidin insertion into a membrane. Gramicidin D is a naturally-occurring mixture of gramicidins A (~85%), B (~10%) and C (~5%) with position 11 (denoted X) being tryptophan, tyrosine or phenylalanine respectively:[46] HCO-L-Val-Gly-L-Ala-D-Leu-L-Ala-D-Val-L-Val-D-Val-L-Trp-D-Leu-L-X-D-Leu-L-Trp-D-Leu-L-Trp-$NH(CH_2)_2OH$. Gramicidin inserts into bacterial membranes and kills bacteria by destroying the ion gradient across the membrane. Although unusual in being a mix of alternating D- and L-isomers, gramicidin is widely used as a model peptide.

The kinetics of gramicidin's insertion has mainly been studied by fluorescence and circular dichroism. Fluorescence gives an indication of the hydrophobicity of the environment of the tryptophans in the peptide. Circular dichroism gives a direct read-out of any changes in secondary structure of the peptide such as its folding into an α-helix. However, neither technique indicates whether the peptide has actually inserted into the membrane. Fluorescence had in fact erroneously been assumed to indicate insertion until a combined CD and LD study showed that gramicidin first inserts its tryptophan residues into the membrane; this is later followed by the backbone folding and inserting.[47,48]

Fig. 19 provides a clear illustration of the effect of the membrane structure on the interaction of a peptide with a membrane. When gramicidin was added to 1,2-dipalmitoyl-*sn*-glycero-3-phosphocholine (DPPC) liposomes at 30 °C (when it is in the more rigid gel phase below the phase transition temperature of 41 °C)[49] a negative LD signal around 234 nm is observed at time $t = 0$ (Fig. 19a). After two hours the tryptophans have reoriented so that their average long axis is perpendicular to the membrane normal. The small signals at low wavelength are consistent with a lack of structure in the peptide backbone and/or a lack of orientation of the peptide backbone relative to the lipid bilayer.

When the experiment was repeated at 50 °C (*i.e.* above the phase transition temperature), the gramicidin LD signal was much larger than that observed at 30 °C (Fig. 19b). The order of magnitude of the LD signal of a lipid-like probe molecule (β-DPH-HPC, 2-(3-(diphenylhexatrienyl)propanoyl)-1-hexadecanoyl-*sn*-glycero-3-phosphocholine) that was part of the membrane is similar at 30 °C and 50 °C, showing that the change is due to the peptide, not due to a change in the

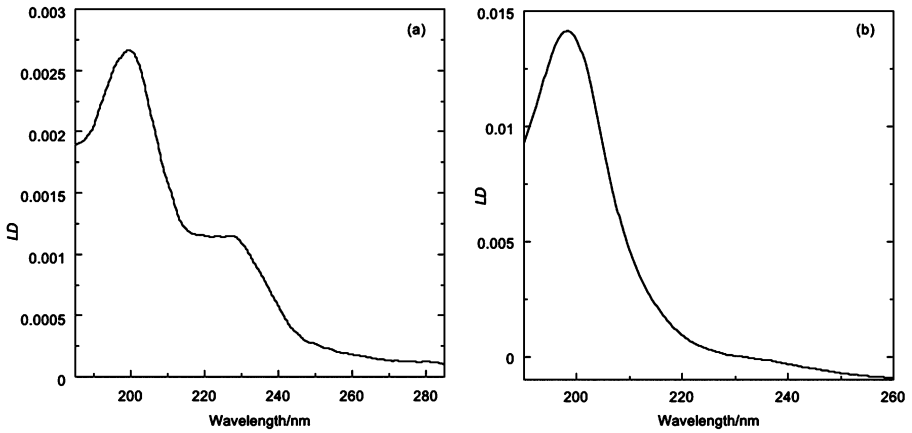

Fig. 17 (a) LD of the α-helical frog peptide aurein 2.5 with sequence: GLFDIVKKVVGAFGSL-NH_2 inserted into a lipid bilayer liposome composed of 50 : 50 DPPC (dipalmitoylphosphatidylcholine) and DPPG (dipalmitoylphosphatidylglycerol) at 50 °C (*i.e.* when in the liquid phase). (b) LD of the β-sheet core peptide fragment GLRILLLKV derived from the T-cell antigen receptor with liposomes made from phosphatidyl choline extracted from soya beans, showing that it sits on the membrane surface. Note the sloping baseline due to the scattering of light by the 100 nm diameter liposomes.

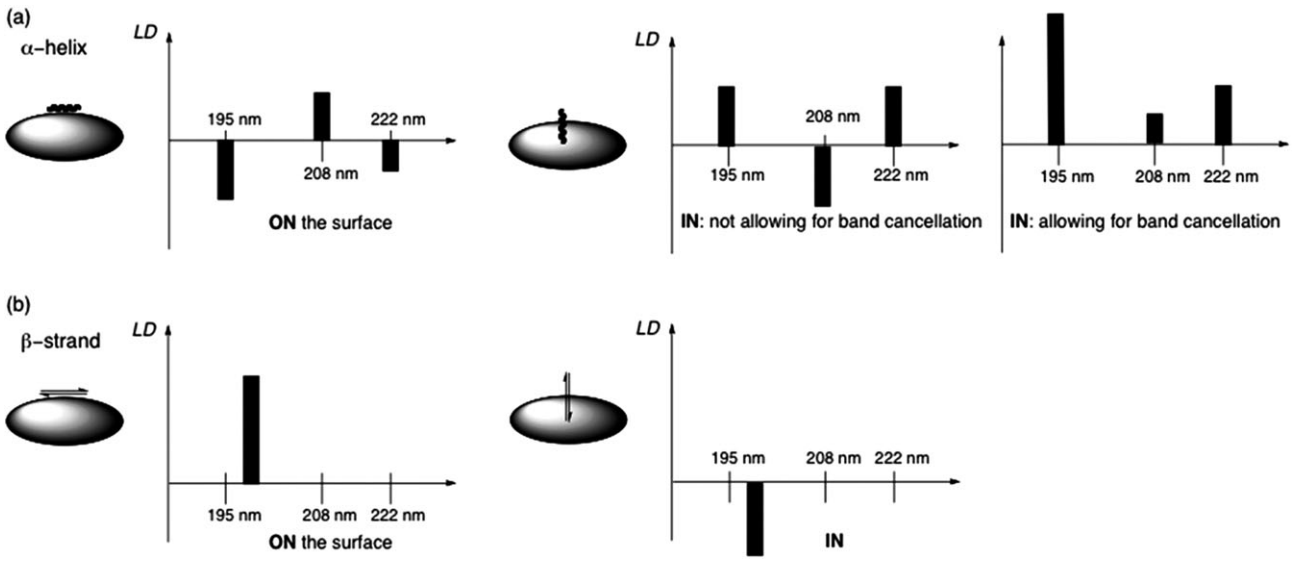

Fig. 18 Schematic illustration of expected LD signals for (a) an α-helix on or in a membrane, and (b) a β-sheet lying flat on the surface of or in a membrane.

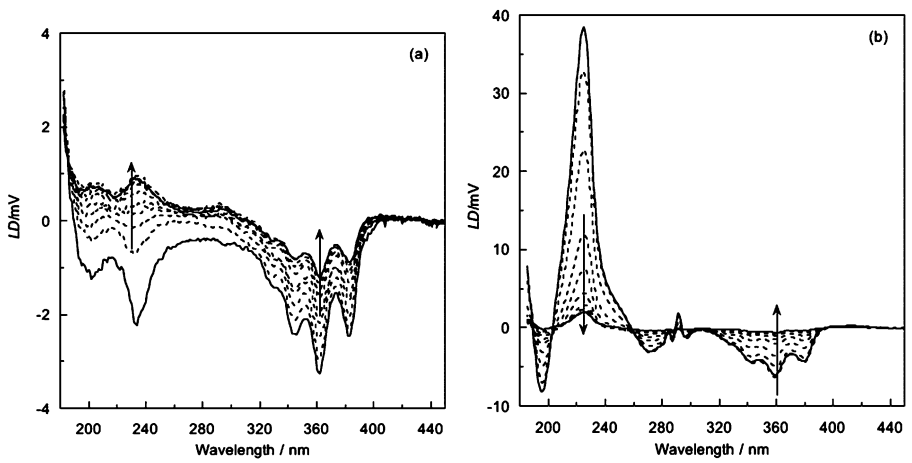

Fig. 19 Kinetics of insertion of gramicidin D into DPPC/β-DPH-HPC (100 : 1 w/w) liposomes at (a) 30 °C and (b) 50 °C. The signal from 300–400 nm is from an additional lipid-like probe molecule. Data were collected at ASTRID[50] synchrotron radiation source on samples with final concentrations of 1 mg ml^{-1} lipid, 0.01 mg ml^{-1} β-DPH-HPC and 0.1 mg ml^{-1} gramicidin in 10% (v/v) TFE using a micro-volume LD cell. Spectra were collected at 12 min intervals. LD = 3.3×10^{-4} per mV.

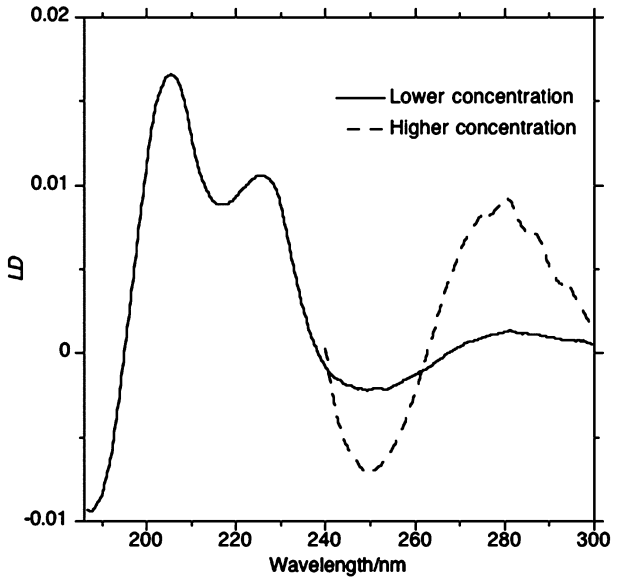

Fig. 20 DNA oriented on carbon M13 phage: atomic level structure[53] together with LD spectra.[54]

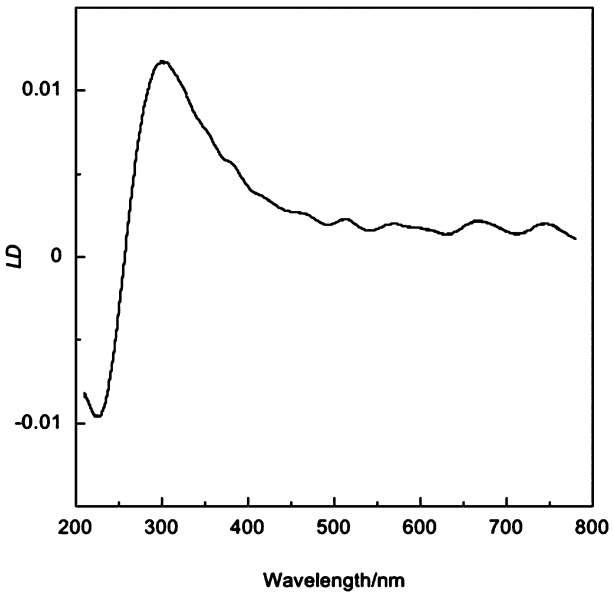

Fig. 21 LD spectra of SWCNTs (1 mg ml^{-1}, 500 μm path length) solubilized by sonicating in aqueous SDS (9 mM).

orientation of the liposomes. The 225 nm band is positive in this case which is consistent with the n to π* backbone transitions being perpendicular to the membrane normal as required for insertion of a helix. The web interface Dichrocalc is being designed to analyse more quantitatively the same transitions in such spectra.[47]

Bacteriophage, the bacterial analogue of viruses

LD methods can be applied to any biomolecule that assembles as a fibre or other asymmetric moiety, perhaps the extreme being that of bacteriophages. Bacteriophages are viruses that infect bacteria. The structure of these viruses is very well understood and consists of an external protein coat enclosing a circular piece of single stranded DNA that encodes the bacteriophage genome. They are an incredibly effective bio-material. Filamentous bacteriophage are a subset of these viruses that have a high aspect ratio, *i.e.* they are much longer than they are wide. Perhaps the best studied and understood filamentous bacteriophage is M13 which is approximately 800 nm in length but only 8 nm in diameter. Filamentous bacteriophage are very rigid having a persistence length in excess of 1000 nm.[51] This makes bacteriophage an ideal object for study by LD.

LD spectra of bacteriophage have very high amplitudes by virtue of the high alignment potential of the particles.[52] The LD signals are further enhanced at higher concentrations because the phage themselves are able to auto-assemble into aligned structures: at high concentrations bacteriophage enter a liquid crystalline phase in which they align with respect to one another to form either smectic or nematic phases. These phases produce a very strong LD signal even when they are simply lain down on quartz plates. Some Couette flow LD spectra are shown in Fig. 20. The phage geometry in a flow LD experiment is analogous to that of membrane proteins in liposomes (so we use eqn (8)).

There are a negative signal in the 190 nm region, positive maxima at 206 and 226 nm and a positive minimum, or more likely a negative maximum, at ~217 nm. These bands are protein dominated. Clack and Gray used phage LD spectra in the 260 nm region to deduce that the tilt of the DNA bases within this phage is greater than 60°.[52] The long wavelength tryptophan signal is very well resolved as a result of the organisation of the tryptophans within the bacteriophage coat.

Nanotubes

Carbon nanotubes (CNTs), a comparatively recently recognized allotrope of carbon,[55] are remarkable materials which are widely studied because of their electronic properties and have a range of potential applications as semi-conductors, catalysts, optical devices, *etc*. Nanotubes are well-ordered hollow graphitic nanomaterials which vary in length from several hundred nanometres to several micrometres and have diameters of 0.4 to 2 nm for single-walled carbon nanotubes (SWCNT). The literature reports a range of molecules binding to SWCNTs, but characterizing the interaction, particularly in solution phase, is challenging.

The LD of SWCNTs shown in Fig. 21 has a large negative LD signal with maximum at 225 nm and a smaller broad positive one at longer wavelength.[56,57] The sign of this signal means that the dominant transition polarization of these SWCNTs lies at more that 54.7° from the nanotube long axis—so across the tube. The positive signals above 260 nm clearly show the electronic transitions are polarized parallel to the nanotubes axis, whilst the negative signals below 260 nm show that some high energy transitions traverse that axis.

Assuming the SWCNT has cylindrical symmetry about its long axis, the ligand-binding geometry is best defined in terms of the normal to the cylinder surface and eqn (8). DNA is widely reported to bind to CNTs and indeed to help solubilise them.[58] The LD of double-stranded calf thymus DNA (that is too short to have a signal of its own) with SWCNTs is shown in Fig. 22. The signal, when that due to the CNT itself is

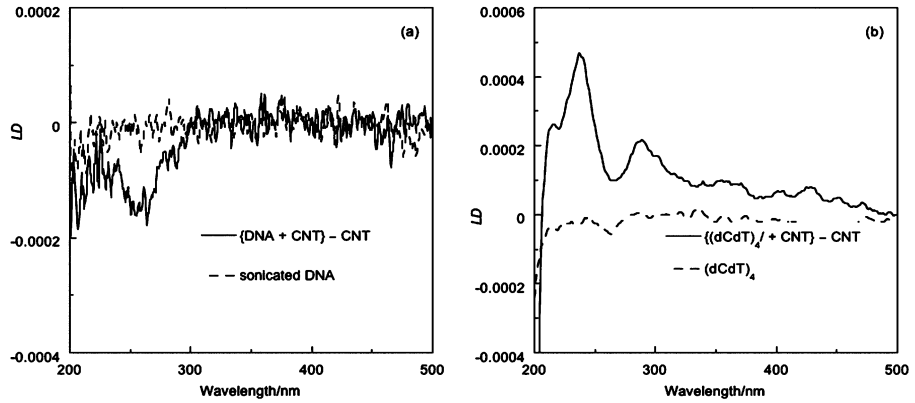

Fig. 22 (a) Difference LD spectrum of SWCNT/sonicated double-stranded DNA complex and SWCNT compared with sonicated DNA (all solutions 0.033 mg ml^{-1}). (b) Difference LD spectrum of single-stranded DNA (dCdT)4/SWCNT and SWCNT compared with (dCdT)4 (all solutions 0.1 mg ml^{-1}).

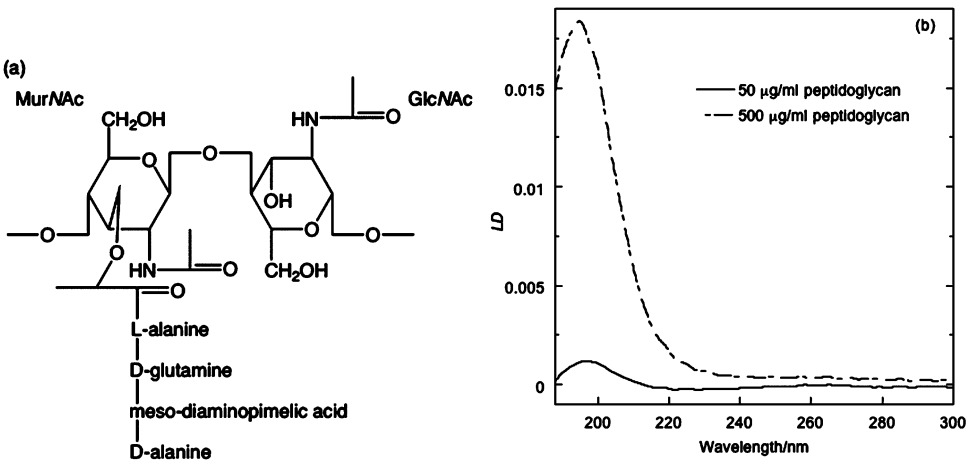

Fig. 23 (a) A primary structure of peptidoglycan, with both types of sugar and a tetrapeptide chain extending from the MurNAc component illustrated. Glc*N*Ac denotes *N*-acetylglucosamine; Mur*N*Ac denotes *N*-acetylmuramicacid. (b) The LD spectra of two concentrations of peptidoglycan as indicated in the figure. Path length was 0.5 mm and the voltage applied to the cell was 3 V.

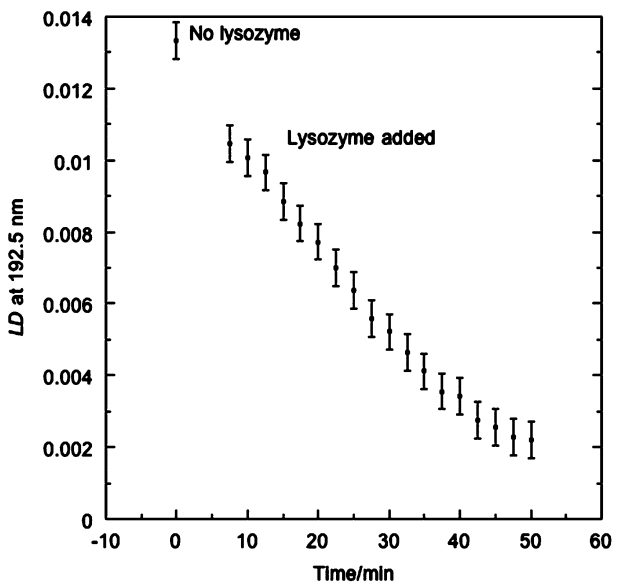

Fig. 24 $LD_{192.5\ nm}$ of peptidoglycan (0.48 mg ml^{-1}) without lysozyme and with lysozyme (0.0097 mg ml^{-1}) as a function of time.[61]

subtracted, is a single negative band at the DNA absorbance maximum; it is similar in shape to a normal DNA LD spectrum such as that of Fig. 9. By way of contrast, the LD spectrum for single stranded DNAs (if they bind to the CNTs) is usually a couplet of bands (Fig. 22) whose position depends on the sequence of the DNA.[56,57]

Peptidoglycan layer of bacterial cells

Bacteria have a barrier separating the interior of the cell from the outside world. This allows transport in and out of the cell to be regulated, and provides some measure of protection from outside attacks. Working from the inside to the outside, the first part of the cell wall is a plasma membrane, a bilayer of phospholipids and proteins that encloses the cytoplasm of the cell. Most bacteria also have a layer of murein, or peptidoglycan, surrounding the plasma membrane helping to maintain the structure and shape of the cell.[59] Some cells have further layers. As the name implies, the peptidoglycan layer is a mixed peptide/sugar complex. The peptidoglycan sacculi from the MC6R41 strain of *E. coli* (which has a defective FtsI gene that

causes it to divide less often at higher temperatures) are rod shaped, making them easily oriented in Couette flow and so excellent subjects for linear dichroism as illustrated in Fig. 23.

Lysozyme is an enzyme that disrupts the murein layer by hydrolysing the β-1–4 link between the GlcNAc and MurNAc sugars on the glycan strands.[60] The peptidoglycan net then becomes disconnected and separates. LD is the ideal technique to follow this process as illustrated in Fig. 24 where the reduction of LD as the peptidoglycan chains gets smaller is apparent.

Conclusions

Flow linear dichroism has a long history with the first Couette flow cell having been designed by Wada in the 1960's. However, it is in recent times that its potential for studying biomaterials has become apparent. In particular the invention of microvolume Couette cells, improved instrumentation, and the discovery that liposomes orient in flow has opened up a wide range of fibre and lipid-based applications that were previously not possible. LD provides structural and kinetic data in solution that are not available from any other technique.

Notes and references

1 P. W. Atkins, *Molecular Quantum Mechanics*, Oxford University Press, Oxford, 1983.
2 P. W. Atkins, *Physical chemistry*, Oxford University Press, Oxford, 4th edn, 1991.
3 J. M. Hollas, *Modern Spectroscopy*, John Wiley and Sons, Chichester, 2nd edn, 1992.
4 D. S. Kliger and J. W. Lewis, *Polarized Light in Optics and Spectroscopy*, Academic Press, Salt Lake City, 1990.
5 J. Michl and E. W. Thulstrup, *Spectroscopy with polarized light*, VCH, New York, 1986.
6 B. Nordén, *Appl. Spectrosc. Rev.*, 1978, **14**, 157–248.
7 A. Rodger and B. Nordén, *Circular dichroism and linear dichroism*, Oxford University Press, Oxford, 1997.
8 B. Nordén, A. Rodger and T. R. Dafforn, *Linear dichroism and circular dichroism*, Royal Society of Chemistry, Cambridge, 2010.
9 A. Jablonski, *Nature*, 1934, **133**, 140.
10 A. Wada, *Biopolymers*, 1964, **2**, 361–380.
11 A. Wada, *Appl. Spectrosc. Rev.*, 1972, **6**, 1–30.
12 R. Marrington, T. R. Dafforn, D. J. Halsall, M. Hicks and A. Rodger, *Analyst*, 2005, **130**, 1608–1616.
13 R. Marrington, T. R. Dafforn, D. J. Halsall and A. Rodger, *Biophys. J.*, 2004, **87**, 2002–2012.
14 M. Ardhammar, N. Mikati and B. Nordén, *J. Am. Chem. Soc.*, 1998, **120**, 9957–9958.
15 A. Rodger, J. Rajendra, R. Marrington, M. Ardhammar, B. Nordén, J. D. Hirst, A. T. B. Gilbert, T. R. Dafforn, D. J. Halsall, C. A. Woolhead, C. Robinson, T. J. Pinheiro, J. Kazlauskaite, M. Seymour, N. Perez and M. J. Hannon, *Phys. Chem. Chem. Phys.*, 2002, **4**, 4051–4057.
16 D. Marsh, M. Muller and F. J. Schmitt, *Biophys. J.*, 2000, **78**, 2499–2510.
17 K. E. Marshall, M. R. Hicks, T. L. Williams, S. V. Hoffmann, A. Rodger, T. R. Dafforn and L. C. Serpell, *Biophys. J.*, 2010, **98**, 330–338.
18 J. Nordh, J. Deinum and B. Nordén, *Eur. Biophys. J.*, 1986, **14**, 113–122.
19 A. Rodger, R. Marrington, M. A. Geeves, M. Hicks, L. de Alwis, D. J. Halsall and T. R. Dafforn, *Phys. Chem. Chem. Phys.*, 2006, **8**, 3161–3171.
20 R. Marrington, M. Seymour and A. Rodger, *Chirality*, 2006, **18**, 680–690.
21 D. J. Gordon and G. Holzwarth, *Arch. Biochem. Biophys.*, 1971, **142**, 481–488.
22 B. Nordén, *Spectrosc. Lett.*, 1977, **10**, 483–488.
23 P. J. Chou and J. W. C. Johnson, *J. Am. Chem. Soc.*, 1993, **115**, 1205–1214.
24 A. Holmén, A. Broo, B. Albinsson and B. Nordén, *J. Am. Chem. Soc.*, 1997, **119**, 12240–12250.
25 L. B. Clark, *J. Phys. Chem.*, 1990, **94**, 2873–2879.
26 L. B. Clark, *J. Am. Chem. Soc.*, 1977, **99**, 3934–3938.
27 F. Zaloudek, J. S. Novros and L. B. Clark, *J. Am. Chem. Soc.*, 1985, **107**, 7344–7351.
28 J. A. L. Williams, C. Cheong, J. I. Tinoco and L. B. Clark, *Nucleic Acids Res.*, 1986, **14**, 6649–6659.
29 Y. Matsuoka and B. Nordén, *Biopolymers*, 1982, **21**, 2433–2452.
30 C. Hiort, B. Nordén and A. Rodger, *J. Am. Chem. Soc.*, 1990, **112**, 1971–1982.
31 K. K. Patel, E. A. Plummer, M. Darwish, A. Rodger and M. J. Hannon, *J. Inorg. Biochem.*, 2002, **91**, 220–229.
32 A. Rodger, A. Parkinson and S. Best, *Eur. J. Inorg. Chem.*, 2001, 2311–2316.
33 A. Rodger, K. J. Sanders, M. J. Hannon, I. Meistermann, A. Parkinson, D. S. Vidler and I. S. Haworth, *Chirality*, 2000, **12**, 221–236.
34 M. J. Hannon, V. Moreno, M. J. Prieto, E. Molderheim, E. Sletten, I. Meistermann, C. J. Isaac, K. J. Sanders and A. Rodger, *Angew. Chem., Int. Ed.*, 2001, **40**, 879–884.
35 I. Meistermann, V. Moreno, M. J. Prieto, E. Molderheim, E. Sletten, S. Khalid, P. M. Rodger, J. Peberdy, C. J. Isaac, A. Rodger and M. J. Hannon, *Proc. Natl. Acad. Sci. U. S. A.*, 2002, **99**, 5069–5074.
36 L. Gårding and B. Nordén, *Chem. Phys.*, 1979, **41**, 431–437.
37 F. Tjerneld, B. Nordén and H. Wallin, *Biopolymers*, 1982, **21**, 343–358.
38 B. Albinsson, M. Kubista, E. Thulstrup and B. Nordén, *J. Phys. Chem.*, 1989, **93**, 6646–6654.
39 R. W. Woody, in *Methods in protein structure and stability analysis*, ed. V. Uversky and E. Permyakov, Nova Science Publishers Inc, New York, 2007, pp. 291–344.
40 R. Marrington, E. Small, A. Rodger, T. R. Dafforn and S. Addinall, *J. Biol. Chem.*, 2004, **279**, 48821–48829.
41 R. Marrington, M. Seymour and A. Rodger, *Chirality*, 2006, **18**, 680–690.
42 E. H. C. Bromley, K. J. Channon, P. J. S. King, Z. N. Mahmoud, E. F. Banwell, M. F. Butler, M. P. Crump, T. R. Dafforn, M. R. Hicks, J. D. Hirst, A. Rodger and D. N. Woolfson, *Biophys. J.*, 2010, **98**, 1668–1676.
43 M. J. Pandya, G. M. Spooner, M. Sunde, J. R. Thorpe, A. Rodger and D. N. Woolfson, *Biochemistry*, 2000, **39**, 8728–8734.
44 T. R. Dafforn, J. Rajendra, D. J. Halsall, L. C. Serpell and A. Rodger, *Biophys. J.*, 2004, **86**, 404–410.
45 C. Dicko, M. R. Hicks, T. R. Dafforn, F. Vollrath, A. Rodger and S. V. Hoffmann, *Biophys. J.*, 2008, **95**, 5974–5977.
46 M. R. Hicks, T. R. Dafforn, A. Damianoglou, P. Wormell, A. Rodger and S. V. Hoffmann, *Analyst*, 2009, **134**, 1623–1628.
47 B. Bulheller, A. Rodger and J. D. Hirst, *Phys. Chem. Chem. Phys.*, 2007, **9**, 2020–2035.
48 M. R. Hicks, A. Damianoglou, A. Rodger and T. R. Dafforn, *J. Mol. Biol.*, 2008, **383**, 358–366.
49 S. Mabrey and J. M. Sturtevant, *Proc. Natl. Acad. Sci. U. S. A.*, 1976, **73**, 3862–3866.
50 C. Dicko, M. R. Hicks, T. R. Dafforn, F. Vollrath, A. Rodger and S. V. Hoffman, *Biophys. J.*, 2008, **95**, 5974–5977.
51 A. S. Khalil, J. M. Ferrer, R. R. Brau, S. T. Kottmann, C. J. Noren, M. J. Lang and A. M. Belcher, *Proc. Natl. Acad. Sci. U. S. A.*, 2007, **104**, 4892–4897.
52 B. A. Clack and D. M. Gray, *Biopolymers*, 1992, **32**, 795–810.
53 Y. A. Wang, X. Yu, S. Overman, M. Tsuboi, G. J. Thomas and E. H. Egelman, *J. Mol. Biol.*, 2006, **361**, 209–215.
54 R. Pacheco-Gomez and T. R. Dafforn, private communication, 2010.
55 M. Monthioux and V. L. Kuznetsov, *Carbon*, 2006, **44**, 1621–1623.
56 J. Rajendra, M. Baxendale, L. G. Dit Rap and A. Rodger, *J. Am. Chem. Soc.*, 2004, **126**, 11182–11188.
57 J. Rajendra and A. Rodger, *Chem.–Eur. J.*, 2005, **11**, 4841–4848.
58 H. Cathcart, V. Nicolosi, J. M. Hughes, W. J. Blau, J. M. Kelly, S. J. Quinn and J. N. Coleman, *J. Am. Chem. Soc.*, 2008, **130**, 12734–12744.
59 W. Vollmer and J.-V. Höltje, *J. Bacteriol.*, 2004, **186**, 5978–5987.
60 D. B. Cordes, A. Miller, S. Gamsey, Z. Sharrett, P. Thoniyot, R. Wessling and B. Singaram, *Org. Biomol. Chem.*, 2005, **3**, 1708–1713.
61 R. Snowdon, unpublished work, 2009.